Measurement and Modeling of Gas Solubility and Literature Review of the Properties for the Carbon Dioxide−Water System

ARTICLE *in* INDUSTRIAL & ENGINEERING CHEMISTRY RESEARCH · MARCH 2004

Impact Factor: 2.59 · DOI: 10.1021/ie034232t

Measurement and Modeling of Gas Solubility and Literature Review of the Properties for the Carbon Dioxide−Water System

A. Chapoy,[†] A. H. Mohammadi,[‡] A. Chareton,[†] B. Tohidi,[‡] and D. Richon*[,†]

Centre d'Energétique, Ecole Nationale Supérieure des Mines de Paris, CENERG/TEP, 35 rue Saint Honoré, 77305 Fontainebleau, France, and Centre for Gas Hydrate Research, Institute of Petroleum Engineering, Heriot-Watt University, Edinburgh EH14 4AS, Scotland, U.K.

New experimental data on the solubility of CO_2 in water are reported in a wide temperature range (i.e., 274.14 up to 351.31 K). The experimental method is based on measurement of the bubble-point pressure of known water−CO_2 binaries at isothermal conditions using a variable-volume *PVT* cell. An extensive literature review has been conducted on the mutual solubilities of CO_2−water systems and CO_2 hydrate-forming conditions. A critical evaluation of the literature data has been conducted to identify any inconsistencies in the reported data. The new experimental data generated in this work are also compared with the literature data, demonstrating the reliability of techniques used in this work. The Valderrama modification of the Patel−Teja equation of state combined with non-density-dependent mixing rules is used to model the fluid phases. The hydrate-forming conditions are modeled by the solid solution theory of van der Waals and Platteeuw with previously reported Kihara potential parameters. The fugacity of ice is calculated by correcting the saturation fugacity of water at the same temperature by using the Poynting correction. The new CO_2 solubility data generated in this work together with the most reliable literature data are used for tuning the binary interaction parameters between subcritical CO_2 and water. The previously reported binary interaction parameters for CO_2 and water are used for the supercritical region. The predicted water content and the hydrate dissociation conditions are compared with the experimental data. The model results are in good agreement with independent experimental data, demonstrating reliability of the techniques and model presented in this work.

1. Introduction

The two main reasons for investigating the thermodynamic properties of carbon dioxide−water systems are the application to the oil and gas industry and CO_2 sequestration. Carbon dioxide and water are often found together in natural gas streams and also in oil reservoirs as part of enhanced oil recovery (EOR). The presence of carbon dioxide and water in these environments may cause complications such as corrosion and hydrate formation. On the other hand, various CO_2 sequestration schemes have generated significant interest in the thermodynamic properties of carbon dioxide−water systems. Accurate knowledge of the behavior of these systems over a wide range of pressures and temperatures is essential for successful application. In particular, reliable solubility data of carbon dioxide in water over a wide range of temperatures and pressures are necessary to develop and validate especially adapted thermodynamic models.

In this work, experimental data on the solubility of carbon dioxide in water and the water content of gaseous carbon dioxide as well as the experimental hydrate dissociation conditions have been assembled from the literature. The main objective was to identify any inconsistency and gap in the available data.

Furthermore, a series of new data on the solubility of carbon dioxide in water have been generated over a wide temperature range. A technique based on measurement of the bubble-point pressure of known CO_2−water binary mixtures at isothermal conditions, using a variable-volume *PVT* cell, has been used in this work.

The Valderrama modification of the Patel−Teja equation of state (VPT-EoS)[1] with non-density-dependent mixing rules (NDD)[2] is used to model the fluid phases. The hydrate phase has been modeled by the solid solution theory of van der Waals and Platteeuw.[3] The fugacity of ice is calculated by correcting the saturation fugacity of water at the same temperature by using the Poynting correction. The binary interaction parameters (BIPs) between subcritical carbon dioxide and water are tuned using the new experimental results on the carbon dioxide solubility in water and the most reliable literature data. Using the new sets of BIPs and the previously reported BIPs for supercritical carbon dioxide and water as well as Kihara potential parameters for carbon dioxide, the water content and hydrate dissociation conditions of carbon dioxide are predicted and compared with the literature data. The predictions are in good agreement with the experimental data, demonstrating the reliability of the experimental technique and thermodynamic modeling used in this work.

2. Review of Experimental Data

2.1. Carbon Dioxide Solubility in Water. Recently, two good reviews on the solubility of carbon dioxide in water have been published.[4,5] The authors have gathered a large number of available experimental data. Diamond and Akinfiev[4] have even developed a semiempirical model for predicting the CO_2 solubility in water.

* To whom correspondence should be addressed. Tel.: +(33) 164694965. Fax: +(33) 164694968. E-mail: richon@paris.ensmp.fr.

[†] Ecole Nationale Supérieure des Mines de Paris.

[‡] Heriot-Watt University.

10.1021/ie034232t CCC: $27.50
Published on Web 03/09/2004

Table 1. List of Reliable Experimental Data for Carbon Dioxide Solubility in Water below 373.15 K

ref	T/K	P/MPa	no. of exptl pts	AAD[a] %	AAD[b] %
		273.15 K < T ≤ 277.13 K			
6	274.15−276.15	0.07−1.42	12	1.54	0.71
7	273.15	1.082	1	0.11	2.77
		277.13 K < T ≤ T_c			
6	278.15−288.15	0.83−2.179	42	1.06	0.94
8	293.15−303.15	0.486−2.986	18	3.01	3.18
9	298.15−302.55	5.07−5.52	2	3.13	1.89
10	283.15−298.15	1−5	7	2.45	2.59
11	298.31−298.57	2.7−5.33	7	2.93	2.47
7	298.15	1.11−5.689	18	1.40	1.83
12	298.15	4.955	3	3.24	3.06
13	298.15	4.955	4	2.38	2.16
14 and 15	291.15−304.19	2.53−5.06	5	0.95	1.55
16	283.15−303.15	0.101−2.027	15	0.86	1.55
17	303.15	0.99−3.891	4	2.35	2.03
		T_c < T ≤ 373.15 K			
9	304.25−366.45	0.69−20.27	13	4.61	4.73
18	323.15−373.15	10−60	9	5.45	2.18
10	323.15−343.15	1−16	16	1.66	2.50
7	323.15−373.15	1.94−9.12	57	2.78	1.86
12	323.15−348.15	4.955	8	1.35	1.41
13	373.15	4.955	3	6.49	2.79
14 and 15	308.15−373.15	2.53−70.9	45	3.38	1.83
17	323.15−353.15	0.993−3.88	9	4.87	1.92
19	323.15−373.15	0.488−4.56	9	3.90	3.42
20	373.15	0.3−1.8	7	10.49	1.01
21	323.15−353.15	4−13.1	29	2.36	1.23

[a] Using VPT-EoS and NDD mixing rules. [b] Using the semiempirical model from ref 4.

This model has been used in screening of the reported literature data. Table 1 shows the literature data with less than 5% average absolute deviation (AAD). In this table, the temperature and pressure ranges, number of data points, statistical analysis, and source of data for the CO_2−water system are reported. These data together with the data generated in this work have been used in tuning BIPs as detailed later. Figure 1 shows the temperatures and pressures of all of the data investigated in this work.

Table 2. List of Experimental Water Content Data for the Carbon Dioxide−Water System below 373.15 K

ref	T/K	P/MPa	no. of exptl pts	AAD %
		277.13 K < T ≤ T_c		
22	298.15−304.19	0.1−5.07	6	2.98
24	298.15	2.27−3.74	5	10.46
26	298.15	3.63	1	5.29
		T_c < T ≤ 373.15 K		
22	323.15−348.15	0.1−70.92	22	4.56
23	323.15−348.15	2.55−30.4	17	5.45
24	323.15−373.15	1.7−5.14	17	4.44
25	323.15	6.82−17.68	7	2.36
27	373.15	0.325−2.307	7	12.87
28	323.15−348.15	10.13−15.2	4	19.59
29	323.15	10.1−30.1	3	10.95

2.2. Water Content in the Gas Phase of the Carbon Dioxide−Water System. A list of experimental data reported in the literature on the water content of the vapor phase has been presented in Table 2 and plotted in Figure 2. The table shows the temperature and pressure ranges, number of data points, statistical analysis, and source of data.

As shown in Figure 2, the variation of the water content in the vapor phase of the CO_2−water system is a function of pressure and temperature. At subcritical conditions, the water content in the vapor phase normally decreases with an increase in the system pressure at constant temperature. However, at supercritical conditions, the same phenomenon is observed up to a certain pressure (e.g., around 8−10 MPa) and then an increase in the system pressure leads to an increase in the water content (Figure 2).

2.3. Phase Equilibria for Carbon Dioxide Hydrates. Carbon dioxide is known to form structure I gas hydrates under the appropriate temperature and pressure conditions. Because carbon dioxide is subcritical at hydrate-forming conditions and has a relatively low vapor pressure, different phases can be found in the hydrate−carbon dioxide−water system: a hydrate phase, a water-rich liquid phase, an ice phase, a carbon dioxide rich vapor phase, and a carbon dioxide rich liquid phase as well as two quadruple points (e.g., Q_1 at 273.1 K and

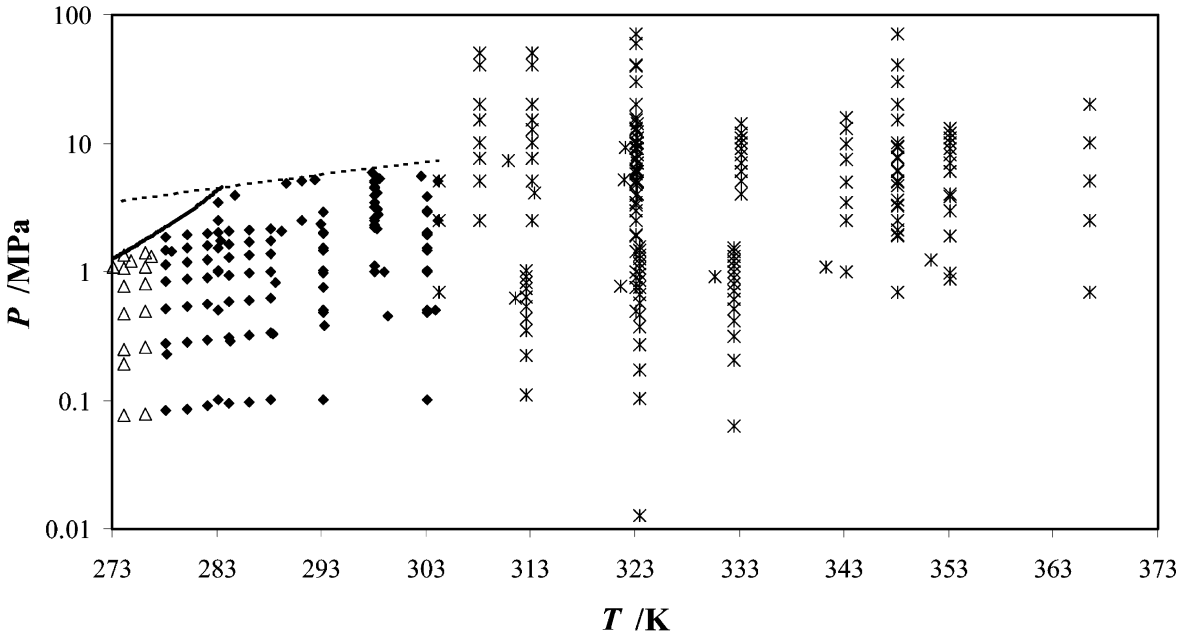

Figure 1. Location of the reliable CO_2 solubility data below 373.15 K in the $P-T$ plan: dashed line, carbon dioxide vapor pressure line; solid line, hydrate dissociation line.

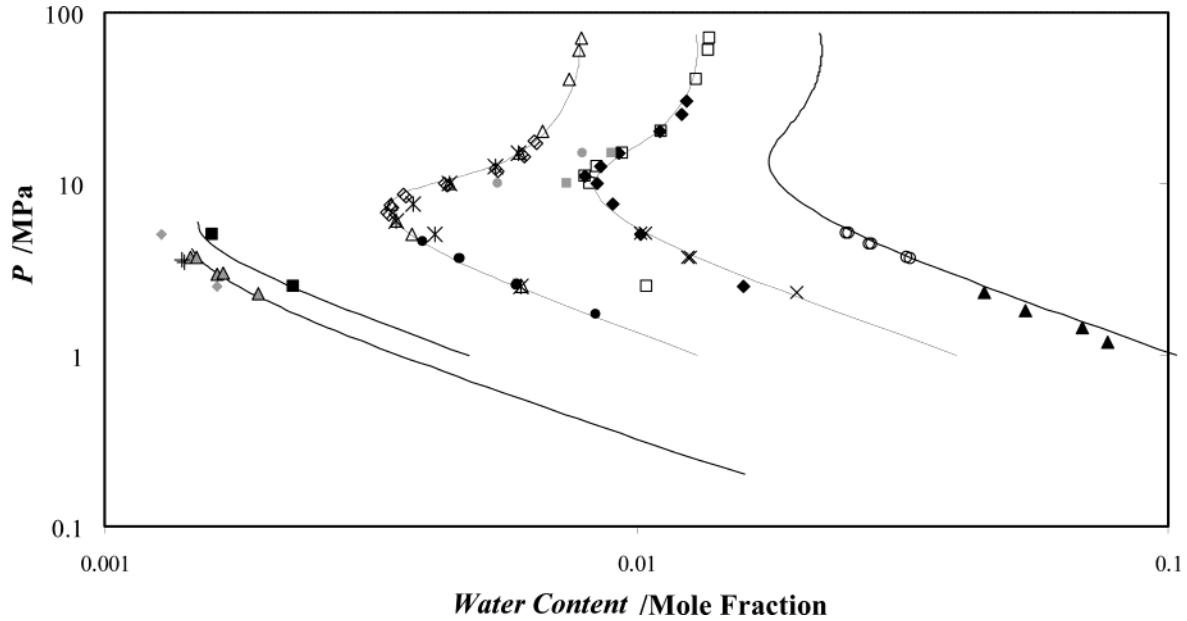

Figure 2. Water content in the gas (or vapor) phase in carbon dioxide−water systems: (gray ◆) 298.15 K from ref 22; (gray ▲) 298.15 K from ref 24; (+) 298.15 K from ref 26; (■) 304.19 K from ref 22; (△) 323.15 K from ref 22; (*) 323.15 K from ref 23; (●) 323.15 K from ref 24; (◇) 323.15 K from ref 25; (gray ●) 323.15 K from ref 28; (□) 348.15 K from ref 22; (◆) 348.15 K from ref 23; (×) 348.15 K from ref 24; (gray ■) 348.15 K from ref 28; (○) 373.15 K from ref 24; (▲) 373.15 K from ref 27; solid curves, predicted with the VPT-EoS[1] and NDD mixing rules.[2]

Table 3. List of Experimental Data for Dissociation Conditions of Carbon Dioxide Hydrates

ref	*T*/K	no. of exptl pts
	Ice−Hydrate−Gas	
30	256.8−271.4	9
31	151.7−192.5	8
32	194.5−217.8	5
	Liquid Water−Hydrate−Gas	
33	273.7−282.9	19
34	277.2−283.1	5
30	271.8−283.2	36
35	273.9−283.2	7
36	279.6−282.8	3
37	271.6−283.2	44
38	274.3−282.9	9
39	274.7−279.7	3
40	276.52−282.5	10
	Liquid Carbon Dioxide−Hydrate−Gas	
30	258.8−285	32
37	263−288	54
	Liquid Carbon Dioxide−Hydrate−Liquid Water	
36	282.9−283.9	6
40	283.33−283.36	2
41	283.2−292.7	15

1.256 MPa and Q_2 at 283 K and 4.499 MPa).[30] Experimental data for carbon dioxide hydrates have been measured and reported by various authors in different hydrate regions. Table 3 gives a list of these data, reporting the temperature range, number of data points, and source of experimental data.

3. New CO_2 in Water Solubility Data and Measurements

3.1. Materials. Carbon dioxide is from Messer Griesheim with a certified purity higher than 99.95 vol %. Distilled and deionized water was used after careful degassing.

3.2. Apparatus and Experimental Procedures. The apparatus used in this work is based on measurement of the bubble-point pressure of various known CO_2−water binaries at isothermal conditions, using a graphical technique. The experimental setup consists of a variable-volume *PVT* cell as described by Fontalba et al.[42] The composition of the system is determined by measuring the exact amounts of water and CO_2 loaded into the cell using an analytical balance with a reported accuracy of 2 mg (up to 2 kg is used). Then the system pressure is increased step by step (by reducing the cell volume) and mixed thoroughly to ensure equilibrium. The stabilized system pressure is plotted versus the cell volume, where a change in slope indicates the system bubble point for the given temperature. The mole fraction of CO_2 in the system is reported as the solubility of CO_2 in water at the given temperature and pressure conditions. The uncertainties in the measured pressure and temperature conditions are within ±0.002 MPa and ±0.1 K, respectively. The experimental gas solubility data are reported in Table 4 and plotted in Figure 3.

Table 4. Experimental Solubility Data of Carbon Dioxide in Water Generated in This Work

T/K	*P*/MPa	x_{CO_2}	*T*/K	*P*/MPa	x_{CO_2}
		273.15 K < *T* ≤ 277.13 K			
274.14	0.190	0.002 62	276.74	1.327	0.014 20
274.83	1.201	0.014 20			
		277.13 K < *T* ≤ T_c			
278.22	0.228	0.002 62	292.35	5.172	0.024 88
278.74	1.426	0.014 20	293.01	2.349	0.014 20
283.38	1.732	0.014 20	293.34	0.385	0.002 62
284.27	0.287	0.002 62	298.40	2.780	0.014 20
284.73	3.938	0.024 88	299.06	1.008	0.005 9
288.41	0.329	0.002 62	299.32	0.452	0.002 62
289.20	2.062	0.014 20	303.99	0.499	0.002 62
289.62	4.844	0.024 88			
		T_c < *T* ≤ 373.15 K			
310.86	7.309	0.020 17	322.14	9.333	0.020 17
311.62	0.630	0.002 62	330.60	0.913	0.002 62
313.36	4.119	0.014 20	341.24	1.086	0.002 62
321.64	0.779	0.002 62	351.31	1.243	0.002 62
321.97	5.216	0.014 20			

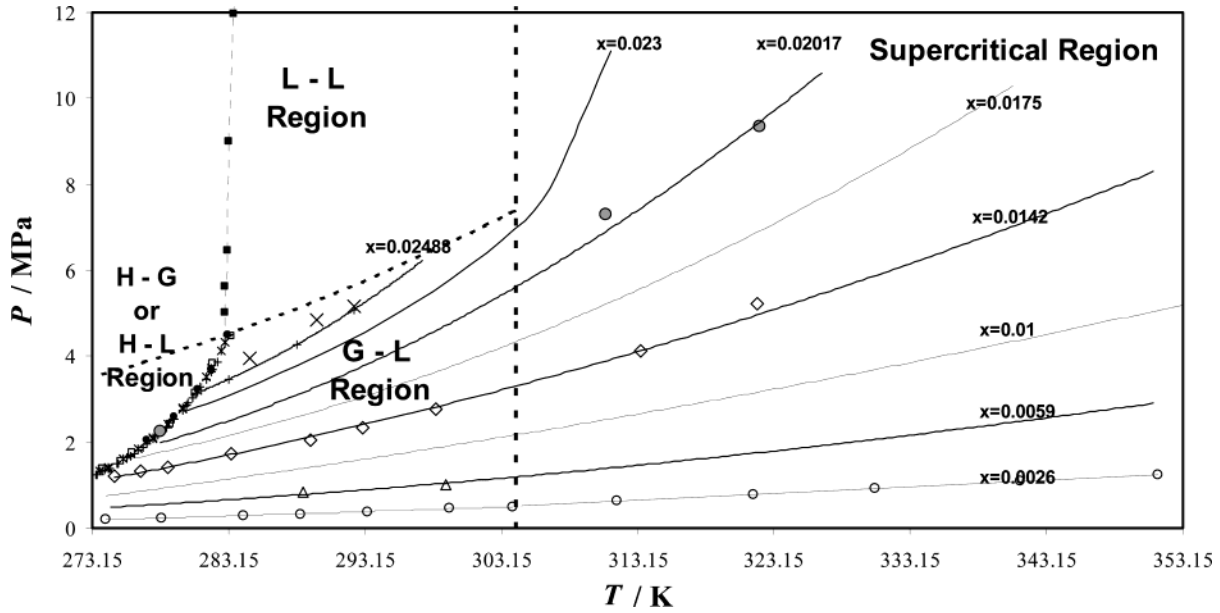

Figure 3. Carbon dioxide solubility data in water from 273.15 to 353.15 K generated in this work: (○) $x_{CO_2} = 0.00262$; (△) $x_{CO_2} = 0.0059$; (◇) $x_{CO_2} = 0.0142$; (gray ●), $x_{CO_2} = 0.02017$; (×) $x_{CO_2} = 0.02488$; solid curves, calculated using the VPT-EoS[1] and NDD mixing rules.[2]

Table 5. Critical Properties and Acentric Factors for Water and Carbon Dioxide

compound	P_c/MPa	T_c/K	v_c/m^3·kgmol^{-1}	ω
water	22.048	647.30	0.056	0.3442
carbon dioxide	7.377	304.20	0.094	0.2276

4. Thermodynamic Modeling

4.1. Pure Compound Properties. The critical temperature (T_c), critical pressure (P_c), critical volume (v_c), and acentric factor (ω) for each of the two pure compounds are provided in Table 5.

4.2. Description of the Model. A general phase equilibrium model based on the uniformity of the fugacity of each component throughout all of the phases[43,44] is used to model the gas solubility, water content, and also hydrate dissociation conditions. In this model, the VPT-EoS[1] with the NDD mixing rules[2] is employed in calculating fugacities in all fluid phases. This combination has proved to be a strong tool in modeling systems with polar as well as nonpolar compounds.[2]

The VPT-EoS is given by

$$P = \frac{RT}{v-b} - \frac{a\alpha(T_r)}{v(v+b)+c(v-b)} \quad (1)$$

with

$$a = \frac{\Omega_a R^2 T_c^{\,2}}{P_c} \quad (2)$$

$$b = \frac{\Omega_b R T_c}{P_c} \quad (3)$$

$$c = \frac{\Omega_{c*} R T_c}{P_c} \quad (4)$$

$$\alpha(T_r) = [1 + F(1 - T_r^{\Psi})]^2 \quad (5)$$

where P is the pressure, T is the temperature, v is the molar volume, R is the universal gas constant, and $\psi = 0.5$. The subscripts c and r denote critical and reduced properties, respectively.

The coefficients Ω_a, Ω_b, Ω_{c*}, and F are given by

$$\Omega_a = 0.66121 - 0.76105Z_c \quad (6)$$

$$\Omega_b = 0.02207 + 0.20868Z_c \quad (7)$$

$$\Omega_{c*} = 0.57765 - 1.87080Z_c \quad (8)$$

$$F = 0.46283 + 3.58230(\omega Z_c) + 8.19417(\omega Z_c)^2 \quad (9)$$

where Z_c is the critical compressibility factor and ω is the acentric factor. Tohidi-Kalorazi[45] relaxed the α function for water, $\alpha_w(T_r)$, using experimental water vapor pressure data in the range of 258.15−374.15 K, to improve the predicted water fugacity:

$$\alpha_w(T_r) = 2.4968 - 3.0661T_r + 2.7048T_r^{\,2} - 1.2219T_r^{\,3} \quad (10)$$

The above relation is used in the present work.

In this work the NDD mixing rules developed by Avlonitis et al.[2] are applied to describe mixing in the a parameter

$$a = a^C + a^A \quad (11)$$

where a^C is given by the classical quadratic mixing rules as

$$a^C = \sum_i \sum_j x_i x_j a_{ij} \quad (12)$$

and b, c, and a_{ij} parameters are expressed by

$$b = \sum_i x_i b_i \quad (13)$$

$$c = \sum_i x_i c_i \quad (14)$$

$$a_{ij} = (1 - k_{ij})\sqrt{a_i a_j} \quad (15)$$

where k_{ij} is the standard BIP.

The term a^A corrects for asymmetric interaction, which cannot be efficiently accounted for by classical mixing rules:

$$a^{\mathrm{A}} = \sum_p x_p{}^2 \sum_i x_i a_{pi} l_{pi} \tag{16}$$

$$a_{pi} = \sqrt{a_p a_i} \tag{17}$$

$$l_{pi} = l_{pi}^0 - l_{pi}^1 (T - T_0) \tag{18}$$

where p is the index of polar components, l_{pi}^0 and l_{pi}^1 are dimensionless constants expected to be positive, and T_0 is the ice point in Kelvin.

Using the VPT-EoS and the NDD mixing rules, the fugacity of each component in all fluid phases is calculated from

$$\ln \phi_i = \frac{1}{RT}\int_V^\infty \left[\left(\frac{\partial P}{\partial n_i}\right)_{T,V,n_{j\neq i}} - RT/V\right] \mathrm{dV} - \ln Z \quad \text{for } i = 1, 2, ..., M \tag{19}$$

$$f_i = x_i \phi_i P \tag{20}$$

where ϕ_i, V, M, n_i, Z, and f_i are the fugacity coefficient of component i in the fluid phases, volume, number of components, number of moles of component i, compressibility factor of the system, and fugacity of component i in the fluid phases, respectively.

The fugacity of ice is rigorously calculated by correcting the saturation fugacity of water at the same temperature by using the Poynting correction:

$$f_{\mathrm{w}}^{\mathrm{I}} = \phi_{\mathrm{w}}^{\mathrm{sat}} P_{\mathrm{I}}^{\mathrm{sat}} \exp\left(\frac{v_{\mathrm{I}}(P - P_{\mathrm{I}}^{\mathrm{sat}})}{RT}\right) \tag{21}$$

where $f_{\mathrm{w}}^{\mathrm{I}}$ is the fugacity of water in the ice phase, $\phi_{\mathrm{w}}^{\mathrm{sat}}$ is the water fugacity coefficient in the vapor phase at pressure equal to the ice vapor pressure, $P_{\mathrm{I}}^{\mathrm{sat}}$ is the ice vapor pressure, and v_{I} is the ice molar volume.

The ice molar volume is calculated using the expression[45]

$$v_{\mathrm{I}} = [19.655 + 0.00224(T - 273.15)]/10^6 \tag{22}$$

where v_{I} and T are in cm^3/g·mol and K, respectively. The ice vapor pressure is calculated using[45]

$$\log(P_{\mathrm{I}}^{\mathrm{sat}}) = -1033/T + 51.06 \log(T) - 0.09771T + 7.036 \times 10^{-5} T^2 - 98.51 \tag{23}$$

where T and $P_{\mathrm{I}}^{\mathrm{sat}}$ are in K and mmHg, respectively.

The fugacity of water in the hydrate phase, $f_{\mathrm{w}}^{\mathrm{H}}$, is given by[46]

$$f_{\mathrm{w}}^{\mathrm{H}} = f_{\mathrm{w}}^{\beta} \exp\left(-\frac{\Delta\mu_{\mathrm{w}}^{\beta-\mathrm{H}}}{RT}\right) \tag{24}$$

where f_{w}^{β} is the fugacity of water in the empty hydrate lattice. $\Delta\mu_{\mathrm{w}}^{\beta-\mathrm{H}}$ is the chemical potential difference of water between the empty hydrate lattice, μ_{w}^{β}, and the hydrate phase, $\mu_{\mathrm{w}}^{\mathrm{H}}$, which is given by the following equation:[3,46,47]

$$\Delta\mu_{\mathrm{w}}^{\beta-\mathrm{H}} = \mu_{\mathrm{w}}^{\beta} - \mu_{\mathrm{w}}^{\mathrm{H}} = RT\sum_m \bar{\nu}_m \ln(1 + \sum_j C_{mj} f_j) \tag{25}$$

where $\bar{\nu}_m$ is the number of cavities of type m per water molecule in the unit cell, f_j is the fugacity of the gas component j, and C_{mj} is the Langmuir constant, which is a function of temperature according to the relation[3,46,47]

$$C_{mj}(T) = \frac{4\pi}{k'T}\int_0^\infty \exp\left(-\frac{w(r)}{k'T}\right) r^2 \, \mathrm{d}r \tag{26}$$

where k' is Boltzmann's constant and $w(r)$ is the spherically symmetric cell potential in the cavity, with r measured from the center and depending on the intermolecular potential function chosen for describing the encaged guest−water interaction. In the present work, the Kihara potential function with a spherical core is used:[47]

$$\Gamma(r) = \infty \qquad r \leq 2\alpha$$

$$\Gamma(r) = 4\epsilon\left[\left(\frac{\sigma^*}{r - 2\alpha}\right)^{12} - \left(\frac{\sigma^*}{r - 2\alpha}\right)^{6}\right] \qquad r > 2\alpha \tag{27}$$

where $\Gamma(r)$ is the potential energy of interaction between two molecules when the distance between their centers is equal to r. ϵ is the characteristic energy, α is the radius of the spherical molecular core, and $\sigma^* = \sigma - 2\alpha$, where σ is the collision diameter, i.e., the distance where $\Gamma = 0$. The Kihara potential parameters, α, σ, and ϵ, are taken from Tohidi-Kalorazi[45] (Table 6). On the basis of the chosen potential energy function, the spherically symmetric cell potential in the cavities (eq 26) needs to be derived. McKoy and Sinanoglu[48] summed up all of these guest−water binary interactions inside the cell to yield an overall cell potential:[47,48]

$$w(r) = 2z\epsilon\left[\frac{(\sigma^*)^{12}}{\bar{R}^{11} r}\left(\delta^{10} + \frac{\alpha}{\bar{R}}\delta^{11}\right) - \frac{(\sigma^*)^{6}}{\bar{R}^{5} r}\left(\delta^{4} + \frac{\alpha}{\bar{R}}\delta^{5}\right)\right] \tag{28}$$

$$\delta^{\bar{N}} = \frac{1}{\bar{N}}\left[\left(1 - \frac{r}{\bar{R}} - \frac{\alpha}{\bar{R}}\right)^{-\bar{N}} - \left(1 + \frac{r}{\bar{R}} - \frac{\alpha}{\bar{R}}\right)^{-\bar{N}}\right] \tag{29}$$

where z is the coordination number of the cavity, that is, the number of gas molecules at the periphery of each cavity, $\bar{R}$ is the cavity radius, r is the distance of the guest molecule from the cavity center, and $\bar{N}$ is an integer equal to 4, 5, 10, or 11.

The fugacity of water in the empty hydrate lattice, f_{w}^{β} in eq 24, is given by[46]

$$f_{\mathrm{w}}^{\beta} = f_{\mathrm{w}}^{\mathrm{I/L}} \exp\left(\frac{\Delta\mu_{\mathrm{w}}^{\beta-\mathrm{I/L}}}{RT}\right) \tag{30}$$

where $f_{\mathrm{w}}^{\mathrm{I/L}}$ is the fugacity of pure ice or liquid water and the quantity inside the parentheses is given by the equation[46,49]

$$\frac{\Delta\mu_{\mathrm{w}}^{\beta-\mathrm{I/L}}}{RT} = \frac{\mu_{\mathrm{w}}^{\beta}(T,P)}{RT} - \frac{\mu_{\mathrm{w}}^{\mathrm{I/L}}(T,P)}{RT} = \frac{\Delta\mu_{\mathrm{w}}^{0}}{RT_0} - \int_{T_0}^{T}\frac{\Delta h_{\mathrm{w}}^{\beta-\mathrm{I/L}}}{RT^2}\,\mathrm{d}T + \int_0^{\mathrm{P}}\frac{\Delta v_{\mathrm{w}}^{\beta-\mathrm{I/L}}}{RT}\,\mathrm{d}P \tag{31}$$

where μ_{w}^{β} and $\mu_{\mathrm{w}}^{\mathrm{I/L}}$ are the chemical potentials of the empty hydrate lattice and of pure water in the ice (I) or the liquid (L) state, respectively. $\Delta\mu_{\mathrm{w}}^{0}$ is the reference

Table 6. Kihara Potential Parameters for Carbon Dioxide−Water Interactions (from Tohidi-Kalorazi[45])

	α/Å	σ^{*} [a]/Å	(ϵ/k')/K
carbon dioxide	0.7530	2.9040	171.97

[a] $\sigma^{*} = \sigma - 2\alpha$.

Table 7. Thermodynamic Reference Properties for Structure I Hydrates

	sI	ref		sI	ref
$\Delta\mu_w^0$/J·mol^{-1}	1297	50	Δv_w/cm^3·mol^{-1} [b]	3.0	47
Δh_w^0/J·mol^{-1} *a*	1389	50	ΔC_{pw}^0/J·mol^{-1}·K^{-1} [c]	−37.32	49

[a] In the liquid water region, subtract 6009.5 J mol^{-1} from Δh_w^0. [b] In the liquid water region, add 1.601 cm^3 mol^{-1} to Δv_w. [c] Values to be used in $\Delta C_{pw} = \Delta C_{pw}^0 + 0.179(T - T_0)$ from ref 49.

chemical potential difference between water in the empty hydrate lattice and pure water in the ice phase at 273.15 K. $\Delta h_w^{\beta-I/L}$ and $\Delta v_w^{\beta-I/L}$ are the molar enthalpy and molar volume differences between an empty hydrate lattice and ice or liquid water. $\Delta h_w^{\beta-I/L}$ is given by the equation[46,49]

$$\Delta h_w^{\beta-I/L} = \Delta h_w^0 + \int_{T_0}^{T} \Delta C_{pw}\, dT \qquad (32)$$

where Δh_w^0 is the enthalpy difference between the empty hydrate lattice and ice, at the ice point and zero pressure. The heat capacity difference between the empty hydrate lattice and the pure liquid water phase, ΔC_{pw}, is also temperature-dependent, and the equation recommended by Holder et al.[49] is used:

$$\Delta C_{pw} = -37.32 + 0.179(T - T_0) \qquad T > T_0 \qquad (33)$$

where ΔC_{pw} is in J mol^{-1} K^{-1}. Furthermore, the heat capacity difference between hydrate structures and ice is set equal to zero. The reference properties used are summarized in Table 7.

5. Discussion

To develop the thermodynamic model, the BIPs between carbon dioxide and water are adjusted directly to all subcritical carbon dioxide solubility data reported in Table 1, and these new solubility measurements through a Simplex algorithm using the objective function FOB are displayed in eq 34:

$$\mathrm{FOB} = \frac{1}{N}\sum_{1}^{N}\left|\frac{x_{i,\mathrm{exp}} - x_{i,\mathrm{cal}}}{x_{i,\mathrm{exp}}}\right| \qquad (34)$$

where N is the number of data points, x_{exp} is the measured solubility, and x_{cal} is the calculated solubility. Two different sets of BIPs have been tuned for this system, one below 277.13 K and one ranging from 277.13 K up to the CO_2 critical temperature. The BIPs between the supercritical carbon dioxide and water are set to those reported by Tohidi-Kalorazi[45] (Table 8). The new generated solubility data sets are well represented with the VPT-EoS and the NDD mixing rules (AAD around 2%) and with the semiempirical model of Diamond and Akinfiev[4] (AAD around 2%). The AADs for all of the references used in this work are summarized in Table 1. The overall AADs for the 298 selected solubility data are 2.1 and 1.8% respectively for this model (including 214 independent data) and the semiempirical model exposed by Diamond and Akinfiev.[4]

Table 8. BIPs between Carbon Dioxide (CO_2) and Water (W) for the VPT-EoS[1] and NDD Mixing Rules[2]

system	k_{W-CO_2}	$l^0_{W-CO_2}$	$l^1_{W-CO_2} \times 10^4$
CO_2−water[a]	0.193 14	0.722 80	26.928
CO_2−water[b]	0.168 60	0.671 36	26.433
CO_2−water[c]	0.196 50	0.723 20	23.740

[a] For 273.15 K < T ≤ 277.13 K. [b] For 277.13 K < T ≤ 304.2 K. [c] Tohidi-Kalorazi.[45]

The developed thermodynamic model was employed to predict the water content of the CO_2 gas (or vapor) phase. The results are presented in Figure 2, demonstrating good agreement with the experimental data. The AADs between the experimental data and the model predictions for all of the references are reported in Table 2. As shown in Figure 2 and Table 2, there are limited data on the water content of the vapor phase

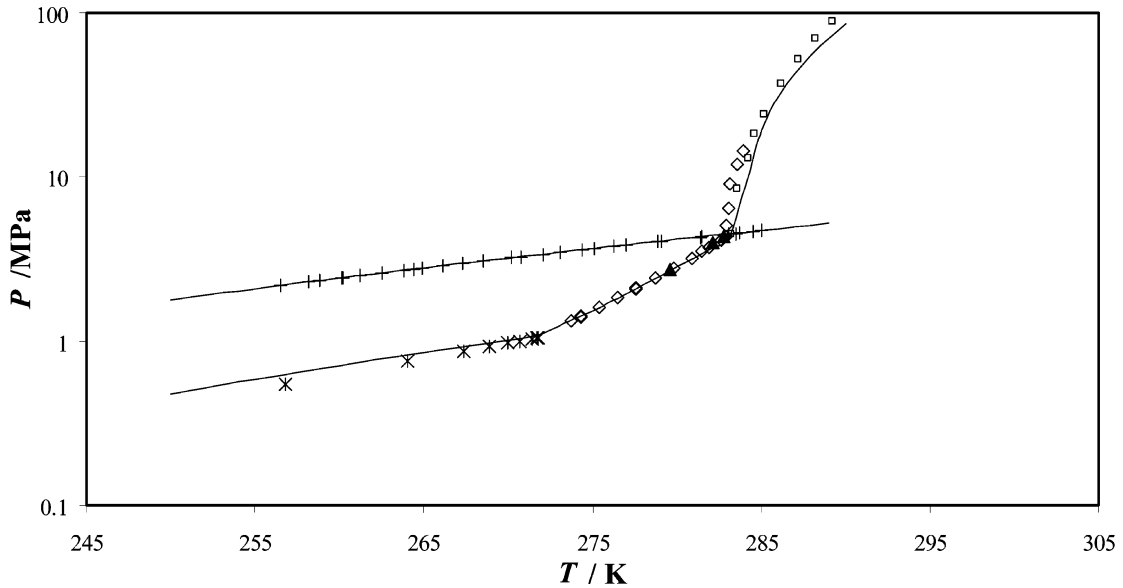

Figure 4. Comparison of experimental and predicted dissociation conditions for CO_2 hydrates: ice−hydrate−gas (*) from ref 30; liquid water−hydrate−gas and liquid water−hydrate−liquid carbon dioxide (◇) from ref 33; (▲) from ref 37; (□) from ref 41; hydrate−liquid carbon dioxide−gas (+) from ref 30.

below the critical temperature of the carbon dioxide. Nevertheless, there is good agreement between the available experimental data and the model predictions.

In the supercritical region, more data have been reported in the open literature. The data reported by Wiebe and Gaddy,[22] Sidorov et al.,[23] Coan and King,[24] and Briones et al.[25] are in good agreement with the model prediction. The data reported by Müller et al.,[27] D'Souza et al.,[28] and Dohrn et al.[29] show some deviations with the model predictions. As shown in Table 2, the data reported by D'Souza et al.[28] have the largest deviation (AAD < 20%).

Figure 4 shows the experimental and predicted phase boundaries for carbon dioxide hydrates. As can be seen, the model predictions are in good agreement with the experimental data collected from the open literature, demonstrating the reliability of the thermodynamic model.

6. Conclusions

Accurate data on the phase equilibria of CO_2−water systems are necessary for a number of processes, including oil and gas transportation, EOR, and CO_2 sequestration. In this work, the following apply:

(i) A comprehensive review of literature data on CO_2−water mutual solubilities, as well as CO_2 hydrate-forming conditions, is reported.

(ii) The paper reports new gas solubility data for CO_2−water systems from low-temperature conditions (near hydrate-forming conditions) up to 351.31 K.

(iii) A technique based on measurement of the bubble-point pressures for known CO_2−water binaries at isothermal conditions has been used in generating the experimental data.

(iv) The experimental gas solubility data at CO_2 subcritical conditions have been used for tuning the BIPs between CO_2 and water in the EoS.

(v) The resulting thermodynamic model has been used for predicting CO_2 solubility in water, as well as the water content of the CO_2 gas (or vapor) phase, and finally CO_2 hydrate phase equilibria over a wide range of temperature and pressure conditions.

(vi) The predictions are in good agreement with the experimental data, demonstrating the reliability of the technique and model used in this work.

Acknowledgment

The financial support by the European Infrastructure for Energy Reserve Optimization (EIERO) provided the opportunity for this joint work, which is gratefully acknowledged.

List of Symbols

AAD = average absolute deviation
BIP = binary interaction parameter
EOR = enhanced oil recovery
FOB = objective function
NDD = non-density-dependent mixing rules
PVT = pressure−volume−temperature
VPT-EoS = Valderrama modification of the Patel−Teja equation of state
C = Langmuir constant
F = parameter of the equation of state
G = gas
H = hydrate
L = liquid
M = number of components
N = number of experimental points
$\bar{N}$ = an integer equal to 4, 5, 10, or 11
P = pressure
Q = quadruple point
R = universal gas constant
$\bar{R}$ = cavity radius
T = temperature
V = volume
Z = compressibility factor
a = attractive parameter of the equation of state
b = parameter of the equation of state
c = parameter of the equation of state
f = fugacity
k = binary interaction parameter for the classical mixing rules
k' = Boltzmann's constant
l = dimensionless constant for the binary interaction parameter for the asymmetric term
n = mole
r = distance
v = molar volume
$\bar{v}$ = number of cavities of type m per water molecule in the unit cell
$w(r)$ = spherically symmetric cell potential function
x = mole fraction
z = coordination number of the cavity

Greek Symbols

Γ = potential energy of the interaction between two molecules
Ψ = power parameter in the VPT-EoS
Ω = parameter in the VPT-EoS
μ = chemical potential
α = hard-core radius
$\alpha(T_r)$ = temperature-dependent function
ϕ = fugacity coefficient
ω = acentric factor
ϵ = characteristic energy
σ = collision diameter
$\sigma^* = \sigma^* = \sigma - 2\alpha$
ΔC_{pw} = heat capacity difference between the empty hydrate lattice and liquid water
ΔC_{pw}^0 = reference heat capacity difference between the empty hydrate lattice and liquid water at 273.15 K
Δh_w = enthalpy difference between the empty hydrate lattice and ice−liquid water
Δh_w^0 = enthalpy difference between the empty hydrate lattice and ice at ice point and zero pressure
Δv_w = volume difference between the empty hydrate lattice and ice
$\Delta \mu_w$ = chemical potential difference between the empty hydrate lattice and ice−liquid water
$\Delta \mu_w^0$ = chemical potential difference between the empty hydrate lattice and ice at ice point and zero pressure
$\Delta \mu_w^{\beta-H}$ = chemical potential difference of water between the empty hydrate lattice and the hydrate phase
$\Delta \mu_w^{\beta-I/L}$ = chemical potential difference of water between the empty hydrate lattice and the ice−liquid water phase

Superscripts

A = asymmetric properties
C = classical properties
H = hydrate
I = ice
L = liquid
sat = saturation conditions
0 = non-temperature-dependent term in the NDD mixing rules
1 = temperature-dependent term in the NDD mixing rules

β = empty hydrate lattice

Subscripts

I = ice
a = index for properties
b = index for properties
c = critical property
c_* = index for properties
cal = calculated property
exp = experimental property
i, j = molecular species
m = type m of cavities
p = index for the polar compound
r = reduced properties
w = water
0 = reference property
1 = first quadruple point
2 = second quadruple point

Literature Cited

(1) Valderrama, J. O. A generalized Patel−Teja equation of state for polar and non-polar fluids and their mixtures. *J. Chem. Eng. Jpn.* **1990**, *23*, 87−91.

(2) Avlonitis, D.; Danesh, A.; Todd, A. C. Prediction of VL and VLL equilibria of mixtures containing petroleum reservoir fluids and methanol with a cubic EoS. *Fluid Phase Equilib.* **1994**, *94*, 181−216.

(3) van der Waals, J. H.; Platteeuw, J. C. Clathrate solutions. *Adv. Chem. Phys.* **1959**, *2*, 2−57.

(4) Diamond, L. W.; Akinfiev, N. N. Solubility of CO_2 in water from −1.5 to 100 °C and from 0.1 to 100 MPa: evaluation of literature data and thermodynamic modeling. *Fluid Phase Equilib.* **2003**, *208*, 265−290.

(5) Spycher, N.; Pruess, K.; Ennis-King, J. CO_2−H_2O mixtures in the geological sequestration of CO_2. I. Assessment and calculation of mutual solubilities from 12 to 100 °C and up to 600 bar. *Geochim. Cosmochim. Acta* **2003**, *67*, 3015−3031.

(6) Anderson, G. K. Solubility of carbon dioxide in water under incipient clathrate formation conditions. *J. Chem. Eng. Data* **2002**, *47*, 219−222.

(7) Zel'vinskii, Y. D. *Zh. Khim. Prom-st.* **1937**, *14*, 1250−1257 (in Russian, cited in ref 4).

(8) Kritschewsky, I. R.; Shaworonkoff, N. M.; Aepelbaum, V. A. *Z. Phys. Chem. A* **1935**, *175*, 232−238 (cited in ref 4).

(9) Gillespie, P. C.; Wilson, G. M. *Vapor−liquid and liquid−liquid equilibria: water−methane, water−carbon dioxide, water−hydrogen sulfide, water−n-pentane, water−methane−n-pentane*; Research Report RR48; Gas Processors Association: Tulsa, OK, 1982.

(10) Oleinik, P. M. Method of evaluating gases in liquids and volumetric properties of solutions under pressure. *Neft. Prom-st., Ser. "Nefte*promysl. *Delo"* **1986** (in Russian, cited in ref 4 and also cited by Namiot, A. Y. *Solubility of gases in water*; Nedra: Moscow, 1991; Vol. 8, p 7 (in Russian)).

(11) Yang, S. O.; Yang, I. M.; Kim, Y. S.; Lee, C. S. Measurement and prediction of phase equilibria for water + CO_2 in hydrate forming conditions. *Fluid Phase Equilib.* **2000**, *175*, 75−89.

(12) Malinin, S. D.; Savelyeva, N. I. The solubility of CO_2 in NaCl and $CaCL_2$ solutions at 25, 50 and 75 °C under elevated CO_2 pressures. *Geochem. Int.* **1972**, *9*, 410−418.

(13) Malinin, S. D.; Kurovskaya, N. A. Investigation of CO_2 solubility in a solution of chlorides at elevated temperatures and pressures of CO_2. *Geochem. Int.* **1975**, *12*, 199−201.

(14) Wiebe, R.; Gaddy, V. L. The solubility in water of carbon dioxide at 50, 75 and 100 °C, at pressures to 700 atm. *J. Am. Chem. Soc.* **1939**, *61*, 315−318.

(15) Wiebe, R.; Gaddy, V. L. The solubility in water of carbon dioxide from 12 to 40 °C and at pressures to 500 atm: Critical Phenomena. *J. Am. Chem. Soc.* **1940**, *62*, 815−817.

(16) Bartholomé, E.; Friz, H. *Chem. Ing. Tech.* **1956**, *28*, 706−708 (cited in ref 4).

(17) Matous, J.; Sobr, J.; Novak, J. P.; Pick, J. Solubilities of carbon dioxide in water at pressure up to 40 atm. *Collect. Czech., Chem. Commun.* **1969**, *34*, 3982−3985.

(18) Shagiakhmetov, R. A.; Tarzimanov, A. A. Deposited Document SPSTL 200 khp-D81-1982, 1981 (cited in ref 4).

(19) Zawisza, A.; Malesinska, B. Solubility of carbon dioxide in liquid water and of water in gaseous carbon dioxide in the range 0.2−5 MPa and at temperatures up to 473 K. *J. Chem. Eng. Data* **1981**, *26*, 388−391.

(20) Müller, G.; Bender, E.; Maurer, G. Das Dampf-Flüssigkeitsgleichgewicht des ternären systems ammonik-kolhendioxid wasser bei hohen wassergehalten im bereich zwischen 373 und 473 K. *Ber. Bunsen-Ges. Phys. Chem.* **1988**, *92*, 148−160.

(21) Bamberger, A.; Sieder, G.; Maurer, G. High-pressure (vapour + liquid) equilibrium in binary mixtures of (carbon dioxide and water or acetic acid) at temperatures from 313 to 353 K. *J. Supercrit. Fluids* **2000**, *17*, 97−110.

(22) Wiebe, R.; Gaddy, V. L. Vapor phase composition of the carbon dioxide-water mixtures at various temperatures and at pressures to 700 atm. *J. Am.Chem. Soc.* **1941**, *63*, 475−477.

(23) Sidorov, I. P.; Kazarnovsky, Y. S.; Goldman, A. M. *Tr. GIAP* **1953**, *1*, 48 (in Russian).

(24) Coan, C. R.; King, A. D. Solubility of compressed carbon dioxide, nitrous oxide and ethane. Evidence of the hydratation of carbon dioxide and nitrous oxide in the gas phase. *J. Am. Chem. Soc.* **1971**, *93*, 1857−1862.

(25) Briones, J. A.; Mullins, J. C.; Thies, M. C.; Kim, B.-U. Ternary phase equilibria for acetic acid−water mixtures with supercritical carbon dioxide. *Fluid Phase Equilib.* **1987**, *36*, 235−246.

(26) Nakayama, T.; Sagara, H.; Arai, K.; Saito, S. High-pressure liquid−liquid equilibria for the system of water, ethanol and 1,1-difluoroethane at 323.2 K. *Fluid Phase Equilib.* **1987**, *38*, 109−127.

(27) Müller, G.; Bender, E.; Maurer, G. Das Dampf-Flüssigkeitsgleichgewicht des ternären systems ammonik-kolhendioxid wasser bei hohen wassergehalten im bereich zwischen 373 und 473 K. *Ber. Bunsen-Ges. Phys. Chem.* **1988**, *92*, 148−160.

(28) D'Souza, R.; Patrick, J. R.; Teja, A. S. High-pressure phase equilibria in the carbon dioxide−*n*-hexadecane and carbon dioxide−water systems. *Can. J. Chem. Eng.* **1988**, *66*, 319−323.

(29) Dohrn, R.; Buenz, A. P.; Devlieghere, F.; Thelen, D. Experimental measurements of phase equilibria for ternary and quaternary systems of glucose, water, carbon dioxide and ethanol with a novel apparatus. *Fluid Phase Equilib.* **1993**, *83*, 149−158.

(30) Larson, S. D. Phase studies of the two-component carbon dioxide water system involving the carbon dioxide hydrate. Ph.D. Thesis, University of Illinois, Urbana-Champaign, IL, 1955.

(31) Miller, S. L. The occurrence of gas hydrates in the solar system. *Proc. Natl. Acad. Sci.* **1961**, *47*, 1798−1808.

(32) Falabella, B. J. A Study of Natural Gas Hydrates. Dissertation, University of Massachusetts, Amherst, MA, 1975.

(33) Deaton, W. M.; Frost, E. M., Jr. Gas hydrate composition and equilibrium data. *Oil Gas J.* **1946**, *45*, 170−178.

(34) Unruh, C. H.; Katz, D. L. Gas-hydrate of carbon dioxide−methane mixtures. *J. Pet. Technol.* **1949**, *1*, 83−86.

(35) Robinson, D. B.; Mehta, B. R. Hydrates in the propane−carbon dioxide−water system. *J. Can. Pet. Technol.* **1971**, *10*, 33−35.

(36) Ng, H. J.; Robinson, D. B. Hydrate formation in system containing methane, ethane, propane, carbon dioxide or hydrogen sulphide in the presence of methanol. *Fluid Phase Equilib.* **1985**, *21*, 145−155.

(37) Vlahakis, J. G.; Chen, H.-S.; Suwandi, M. S.; Bardhum, A. J. The growth rate of ice crystals: Properties of carbon dioxide hydrate, a review of 51 gas hydrates. Syracuse University Research and Development Report 830; U.S. Department of the Interior: Washington, DC, Nov 1972.

(38) Adisasmito, S.; Sloan, E. D., Jr. Hydrates of hydrocarbon gases containing carbon dioxide. *J. Chem. Eng. Data* **1992**, *37*, 343−349.

(39) Fan, S. S.; Guo, T. M. Hydrate formation of CO_2-rich binary and quaternary gas mixtures in aqueous sodium chloride solutions. *J. Chem. Eng. Data* **1999**, *44*, 829−832.

(40) Mooijer-van den Heuvel, M. M.; Witteman, R.; Peters, C. J. Phase behaviour of gas hydrates of carbon dioxide in the presence of tetrahydropyran, cyclobutanone, cyclohexane and methylcyclohexane. *Fluid Phase Equilib.* **2001**, *182*, 97−110.

(41) Takenouchi, S.; Kennedy, G. C. The binary system H_2O−CO_2 at high temperatures and pressures. *Am. J. Sci.* **1964**, *262*, 1055−1074.

(42) Fontalba, F.; Richon, D.; Renon, H. Simultaneous determination of vapor-liquid equilibria and saturated densities up to 45 MPa and 433 K. *Rev. Sci. Instrum*. **1984**, *55*, 944−951.

(43) Avlonitis, D. Thermodynamics of Gas Hydrate Equilibria. Ph.D. Thesis, Heriot-Watt University, Edinburgh, Scotland, 1992.

(44) Tohidi, B.; Burgass, R. W.; Danesh, A.; Todd, A. C. Hydrate inhibition effect of produced water, Part 1. Ethane and propane simple gas hydrates. *SPE 26701, Proc. SPE Offshore Eur. 93 Conf.* **1993**, 255−264.

(45) Tohidi-Kalorazi, B. Gas Hydrate Equilibria in the Presence of Electrolyte Solutions. Ph.D. Thesis, Heriot-Watt University, Edinburgh, Scotland, 1995.

(46) Anderson, F. E.; Prausnitz, J. M. Inhibition of gas hydrates by methanol. *AIChE J*. **1986**, *32* (8), 1321−1332.

(47) Parrish, W. R.; Prausnitz, J. M. Dissociation pressures of gas hydrate formed by gas mixture. *Ind. Eng. Chem. Process Des. Dev*. **1972**, *11*, 26−34.

(48) McKoy, V.; Sinanoglu, O. Theory of dissociation pressures of some gas hydrates. *J. Chem. Phys.* **1963**, *38* (12), 2946−2956 (cited in ref 47).

(49) Holder, G. D.; Corbin, G.; Papadopoulos, K. D. Thermodynamic and molecular properties of gas hydrate from mixtures containing methane, argon and krypton. *Ind. Eng. Chem. Fundam*. **1980**, *19*, 282−286.

(50) Dharmawardhana, P. B.; Parrish, W. R.; Sloan, E. D. Experimental thermodynamic parameters for the prediction of natural gas hydrate dissociation conditions. *Ind. Eng. Chem. Fundam*. **1980**, *19*, 410−414.

Received for review November 3, 2003
Revised manuscript received January 29, 2004
Accepted February 3, 2004

IE034232T